ADVANCES IN MATERIALS SCIENCE, Vol. 24, No. 3 (81), September 2024

DOI: 10.2478/adms-2024-0018

Belkacem Edeb[1], Naas Allout[2,3], Mahmoud Benkhelil[4], Salim Guettala[2,5*]

[1] Architecture Department, Benyoucef Benkhedda University of Algiers 1, Algiers, Algeria
[2] Civil Engineering Department, University of Djelfa, Djelfa, Algeria
[3] Laboratory of Mechanical and Materials Development, University of Djelfa, Djelfa, Algeria
[4] Laboratory Built in Environment, Faculty of Civil Engineering USTHB, Algiers, Algeria
[5] Civil Engineering Research Laboratory, University of Biskra, Biskra, Algeria

** s.guettala@univ-djelfa.dz*

OPTIMIZING HIGH-PERFORMANCE CONCRETE PROPERTIES CONTAINING BLAST FURNACE SLAG AND MARBLE POWDER

ABSTRACT

Building and industrialization-related environmental harm is becoming an increasingly serious concern. In an effort to create an eco-friendly high-performance concrete (HPC), this paper addresses the idea of partially replacing cement with recyclable industrial waste. The current study will experimentally examine the slump, the strengths of compressive (SC) and porosity (P) of fifteen HPC mixtures manufactured from locally available resources. Hence, the effects of utilizing marble powder (MP) as a mineral additive in binary mixes and ternary with cement (PC) and granulated ground blast furnace slag (GGBFS) on the HPCs properties were studied in order to develop statistical models based on mixture design. Highly accurate prediction graphs and models were created for HPC workability, P at 28-day, SC at 7 and 28-day. All responses have satisfactory coefficients of correlation ($R^2 \geq 0.76$). Replacing cement with GGBFS causes a rise in slump in mixtures. Nevertheless, that only remains relevant when the mixtures have a small MP percentage ($\leq 25\%$). A minor decrease in SC can be attributed by an increase of GGBFS. After 28-day, using GGBFS alone caused a little drop in SC; however, when GGBFS and PC were mixed, SC increased, in comparison with reference composition, and the porosity was reduced. Conversely, SC is superior with lower porosity when a small amount of MP is utilized. The best combination is HPC14, containing 5% GGBFS; it offers an optimal equilibrium among the three qualities; with HPC4's (15%GGBFS+5%MP) qualities, being almost identical to those of reference HPC15, a lower amount of cement may also be utilized. Findings encourage the use of MP and GGBFS to partially replace cement to produce eco-friendly and cost-effective HPC. An extremely high correlation coefficient indicated a strong relationship between P and SC.

Keywords: *blast furnace slag; marble powder; HPC; workability; compressive strength; porosity*

INTRODUCTION

The utilization of industrial waste in concrete manufacturing has been a major driver in the development of ecologically friendly construction materials in recent years. Because of this, it is imperative that the high-performance concrete (HPC) composition makes the best use possible of both traditional and, more importantly, alternative resources, namely waste and industrial by-

Received: 2024.07.02; Received in revised form: 2024.09.03; Accepted: 2024.09.03

products. The most crucial ingredient in the creation of HPC is cement; in this case, to further enhance performance by minimizing porosity and creating a strong microstructure, cement can further be produced by combining supplemental cementitious materials (SCMs) with cement [1]. Several investigations have shown that incorporating ultrafine nanomaterials can effectively increase the compactness and binding impact of cementitious materials [2,3]. It is essential to keep in mind that the water/binder ratio must be smaller than 0.4 during design and that the compressive strength of HPC needs to be in excess of 50 MPa after 28 days [4]. The implementation of HPCs is generally made easier by their great fluidity [5].Preserving natural resources and reducing pollution are the primary goals in minimizing the industry's environmental impact. The high demand for concrete, while reducing energy consumption and CO_2 emissions, workable alternatives must be developed [6].To reduce the environmental impacts of cement production and its use in concrete, industrial wastes, such as blast furnace slag and marble powder, have been effectively used as additives for partial substitutes. Granulated ground blast furnace slag (GGBFS) is a very interesting addition to the concrete sector, which has several properties (chemical structure similar to PC, stability of aspects for the same origin, latent reactivity that becomes active when PC is present). Clinker serves as the primary GGBFS activator in GGBFS cements. However, clinker hydrates, such as CH and C-S-H, will be the first to form. The surplus of hydrated lime then causes the GGBFS hydration to be activated, producing hydrated tricalcium aluminates and hydrated calcium silicates, which enhance compressive strength considerably and have a C-S-H texture equivalent to cement. The GGBFS is frequently applied to concrete for improving its strength and durability [7]. There is, nevertheless, a desirable GGBFS percentage. Raising the amount of GGBFS will not appreciably improve the concrete strength over a particular ratio. In order to decrease porosity and increase the mechanical strengths of the concrete, GGBFS is a very helpful solution. It is also very beneficial to the environment and the economy. Because GGBFS significantly reduces initial strength, in numerous cement manufacturers, it has already been utilized as a mineral ingredient, where its dosage was typically regulated between 20 and 25% as a cement alternative. Using a cheap by-product to enhance the properties and durability of concrete has benefits [8]. Furthermore, GGBFS can improve the compressive strength of HPC and offer a significant impact on workability, as reported by Wang et al. [9]. As GGBFS fineness increases, binding activity rises as well. Previous research findings [10,11] indicate that using GGBFS enhances not only the workability or slump of the concrete, but also its mechanical strengths and durability. Although pozzolanic materials can reduce manufacturing costs, save energy, and have fewer adverse effects on the environment, they are gaining interest among academics [12]. Significant cost savings can also be obtained by using GGBFS as a binder component used for the manufacture of concrete [13]. According to Mhaya et al. [14], adding 20% GGBFS to rubberized concrete enhances its mechanical properties, while decreasing its workability. Ganesh and Murthy [15] have demonstrated that replacing more than 20% of cement with GGBFS considerably reduces the strengths. Another study found that adding GGBFS up to 20% increased the concrete compressive and tensile strength; however, adding more GGBFS decreases fluidity, which increases the concrete permeability [16] and reduces its ability to withstand a chemical assault [17]. The micro-filling properties of GGBFS fill the spaces between the components of the concrete, creating a more compact mass that raises the concrete density [16]. Srikanth et al. [18] showed that adding 30% GGBFS to PC decreased porosity, sorptivity, and permeability in HPC and increased its compressive strength by 60% to 70%. On the other hand, waste marble powder is an inert substance that is produced as an industrial byproduct when marble is sawed, shaped, and polished. It poses a significant environmental hazard. Repurposing waste marble to replace some of the cement or aggregate in mortars can serve a dual purpose: it can give new life to this by-product, while also mitigating the environmental impact it causes, to some extent, all without significantly compromising the mechanical properties of mortars [19]. According to Vardhan et al. [20], 20-30% of the marble industry's overall production is made up of waste marble. Seventy percent of marble is lost in Algeria during the extraction, processing, and polishing phases, as reported by Hebhoub et al. [21]. The waste product in question presents noteworthy environmental issues, including soil fertility and morphology, air pollution, canal obstruction, and disposal concerns. A useful and effective technique to close the gap between production and consumption, support environmental preservation, and aid in sustainable development is through the valorization of marble powder (MP) in concrete manufacturing. In the opinion of Ergün [22], adding 5% MP to concrete enhances its compressive strength by 12%. Other researchers [18,23] have also noted this strength improvement. According to Ergün [22] and Chawla et al. [24], the production of carbo-aluminates in the presence of MP, which has binding potential, is responsible for improving the mechanical properties of concrete containing MP. Vardhan et al. [20] noted that when marble content increased, concrete mixes became less workable. The MP primarily provided a filler effect in concrete, according to Aliabdo et al. [25] study into the properties of concrete that had various substitution ratios of MP for sand and cement. By partially substituting MP for cement, Kumar et al. [26] were able to examine the mechanical properties and microstructure of concrete. They found that although MP caused a filling effect at fewer replacement levels; it additionally enhanced the pore structure and increased strength when 5% of cement was replaced with MP. When the replacement rate of MP surpasses 10%, there is a considerable change in the strength of compression, tensile strength, and flexural strength; the strength decreases as the replacement rate rises [27].According to earlier research, 10% of cement can be substituted with MP to achieve the ideal compressive strength and improve the overall mechanical characteristics of concrete [28,29].Findings published in reference [30] indicate enhancements in the fresh and hardened characteristics of SCC made with 10% MP and 30% GGBFS. The utilization of waste that may cause environmental problems is made possible through the use of MP and GGBFS in the manufacturing of SCC, which further enhances its performance. In order to conduct as few tests as feasible, the statistical modeling approach of mixture design enables the determination of the relative relevance of the mixture initial variables and the effects of their interaction with one another on the features under study [31,32]. It also makes the test procedure more logical and aids in modeling the responses (properties) discovered through empirical investigation [33]. In recent years, the mixture design is widely utilized for mixing SCMs with cement due to its rapidity and simplicity of usage [34,35].

In short, the current study aims to promote the use of locally available resources for HPC production. Specifically, applying mix design, investigate the combined impact of MP and GGBFS on the physico-mechanical properties of HPC is a subject that has not received much attention in the literature. In this regard, the modeling technique used in this study is intended for mix design to analyze the impact of using MP as SCM on the workability (slump),porosity accessible to water (P) at 28 days and the strengths of compression (SC) of HPCs at 7 and 28-day; using PC and GGBFS in binary and ternary mixes. This involves predicting the properties of HPCs produced from locally available resources, optimizing them, and creating a perfect mix design that offers an ideal equilibrium among the three qualities.

MATERIALS AND PROCEDURES

Materials characterization

A white composite Portland cement CEM II/A of class 52.5 MPa was utilized with around 12 percent of limestone fillers. Table 1 displays its mineralogical, chemical, and physico-mechanical properties of cement.

Table 1. *Raw material properties: chemical, mineralogical and physico-mechanical*

Chemical composition of cement and mineral additions *(Note: LOI: Loss on ignition)*											
Component (in %)	SiO_2	Al_2O_3	Fe_2O_3	CaO	MgO	SO_3	Na_2O	K_2O	Cl	TiO_2	LOI
PC	23.50	3.30	0.22	63.70	0.70	2.20	0.40	0.50	-	-	4.70
MP	1.00	0.20	0.20	52.60	2.10	0.07	0.06	0.04	-	0.01	43.63
GGBFS	39.60	9.73	3.56	41.20	3.38	0.67	0.01	0.50	0.01	-	1.30
Cement mineralogical composition (%)											
C_3S			C_2S			C_3A			C_4AF		
55.00			23.49			8.37			0.67		
Physico-mechanical properties of cement											
Specific density (kg/m^3)						3120					
Fineness (cm^2/g)						4950					
Normal consistency (%)						25					
Strength of compressive (MPa)				2 days					30.69		
				28 days					57.51		

Using the Bogue procedure [36], the mineralogical composition was determined. MP and GGBFS, two mineral additions, were employed in this investigation. The MP used is the result of cutting pieces of marble in a marble factory workshop in Algeria's Biskra region, and its fineness was roughly 5500 cm^2/g. Table 1 displays the chemical properties of MP; 2700 kg/m^3 is its specific density. Calcite ($CaCO_3$) is the dominant element in the marble powder, according to the X-ray diffraction spectrum of MP displayed in Figure 1.

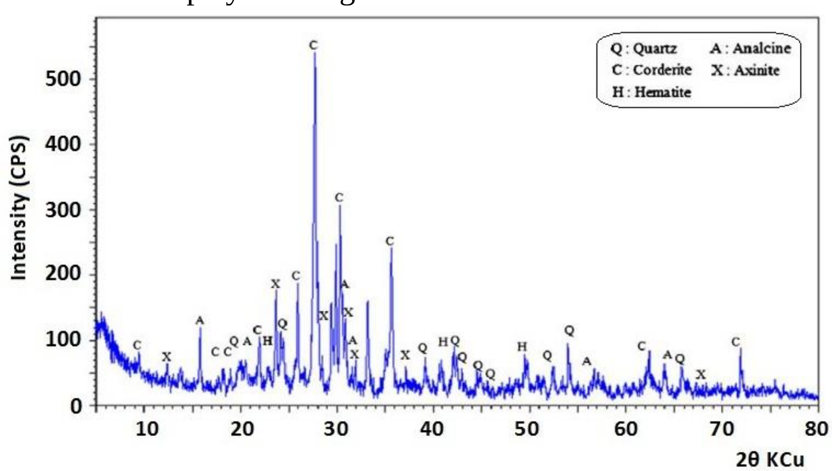

Fig. 1. X-ray diffraction of marble powder

This corresponds to what was found by Chaidet al. [37]. This GGBFS which is a by-product of casting iron production, from the El-hadjar facility in the Algerian province of Annaba, was finely ground to a fineness of roughly 3350 cm^2/g. It has a specific density of 2630 kg/m^3. Table 1 and Figure 2 display chemical properties and X-ray diffraction spectrum of GGBFS, respectively.

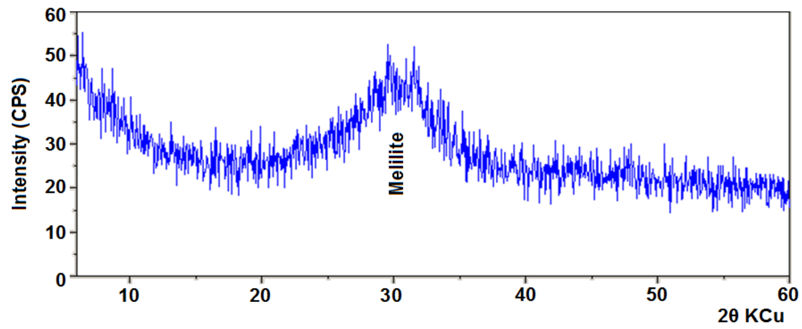

Fig. 2. X-ray diffraction of granulated ground blast furnace slag

Figure 2 reveals that the GGBFS has an amorphous structure that produced a halo in the center that corresponds to the melilite mainline. This is in agreement with the findings of Arroudj et al. [38]. The physical properties of the sand (0/5 mm) in the Djelfa region of Algeria are listed in Table 2. Figure 3 depicts its particle size graph. Two gravels obtained from the Djelfa region (3/8 mm and 8/12.5 mm) were employed. Table 2 and Figure 4 illustrate their physical properties and particle size curves, respectively. Tap water was utilized for both mixing and curing samples. The superplasticizer admixture known as "MEDAFLOW 30" was utilized; it was made by the Algerian company Granitex. The density, dry extract and pH of the superplasticizer are, in this order, 1.05, 30% and 6.

Table 2. *Gravels and sand physical properties*

Characteristic	S 0/5	G 3/8	G 8/12.5
Specific density (kg/m^3)	2620	2660	2640
Coefficient of Los Angeles (%)	-	24.50	24.00
Fines < 80 µm (%)	0.65	-	-
Finesses modulus (FM)	2.79	-	-
Sand equivalent (%)	81.00	-	-

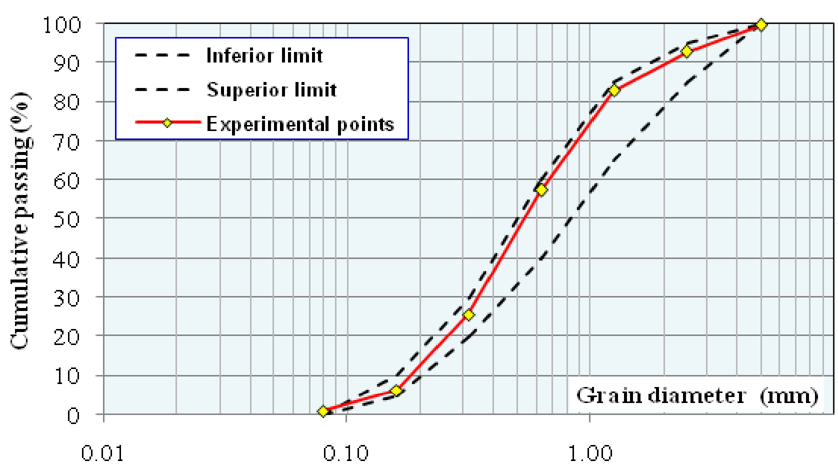

Fig. 3. Sand granulometric curve

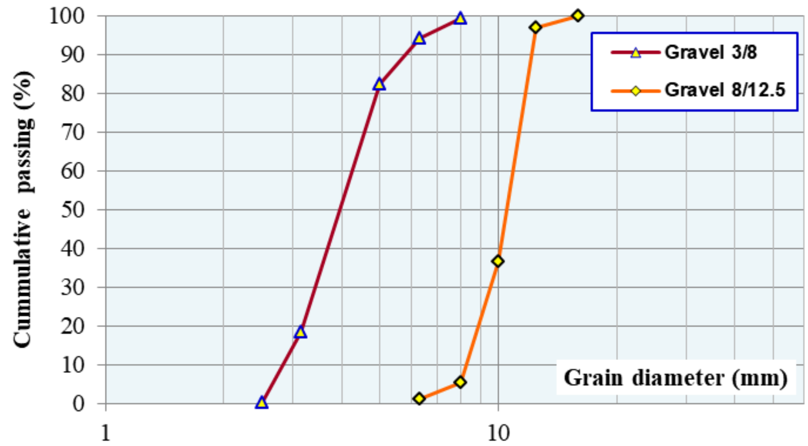

Fig. 4. Gravels granulometric curves

Mixture design technique

Designs of mixture have been employed to more effectively arrange studies that support scientific study when assessing items with numerous components [39]. With a relatively small number of tests, this novel technique improves mixtures. The objective was finding out which law governs one or more responses based on the mixture's composition. PC, GGBFS and MP are the mixture parameters, meaning that each component concentrations (xi) affect one or more properties (responses) (Y), such as the porosity of HPC, the compressive strengths, and slump. Hence, implementing this technique for examining a function of format:

$$Y = f(x_i) \tag{1}$$

By calculating the concentrations, the equation is obtained:

$$\sum_{i=1}^{i=n} x_i = 100\% \tag{2}$$

When the total of the concentrations reaches one, Eq. (2) takes the following form:

$$\sum_{i=1}^{i=n} x_i = 1 \tag{3}$$

The mix design modeling technique is predicated on this formula. The models of mathematical have undergone substantial modifications and the graphical representations of mix design are different from those employed in traditional experimental designs. An equilateral triangle is employed to represent a blend of three parts.

Proportions of mixture

This section considers a three-parameter mix design that takes mass ratios into account (PC, GGBFS, and MP).The sum of these ratios must constantly equal one. The experimental scope is to replace twenty percent of the cement (90 kg); this is equivalent to one-fifth of the quantity.

There were limitations to this experimental scope, including:

$$PC + GGBFS + MP = 1 \tag{4}$$

Experiments number (C) can be computed using the following formula:

$$C_{q+m-1}^{m} = \frac{(q+m-1)!}{(m)!(q-1)!} \tag{5}$$

Where: (q) is the number of parameters; (m) is the number of levels.

There are fifteen experiments that must be managed according to 3 parameters and 4 levels. A mathematical model that characterizes the different effects (PC, GGBFS, MP, and the binary mixes and ternary of PC, GGBFS, and MP) on a particular characteristic can be created. A second-degree polynomial model including 4 levels and 3 non-independent parameters (PC, GGBFS, and MP) was utilized. The following is the presentation of the statistical model:

$$Y = c_1 \times PC + c_2 \times GGBFS + c_3 \times MP + c_{12} \times (PC.GGBFS) + c_{13} \times (PC.MP) + c_{23} \times (GGBFS.MP) \tag{6}$$

Where: themodel's coefficients are ($c_1, c_2, c_3, c_{12}, c_{13}, c_{23}$); the response is ($Y$).

These coefficients show the impact of each component and the interplay of elements on the characteristic "response". Although these coefficients are not known, the values of these coefficients should be extracted from the experiment findings using the standard least-squares fitting technique. The residuals were employed for evaluating and determining the coefficients variance in order to assess each term's importance within the model [39]. Figure 5 shows an equilateral triangle with fifteen compositions using the three parameters. The ratios of the parameters in the formulations under examination, as provided by the software, are shown in Table 3.The slump, P at 28 days and SC at 7 and 28 days of HPCare the expected responses. The responses that have been provided are then analyzed using the JMP7 statistical software. Iso-response curves, or ternary diagrams, create a relationship between the three parameters and depict the responses under discussion.

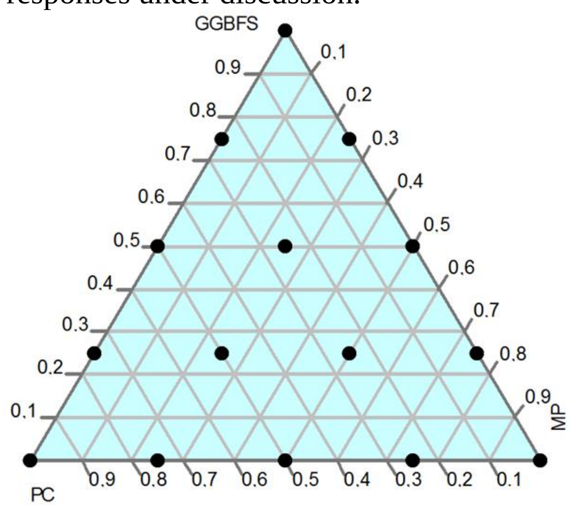

Fig. 5. Fifteen compositions were examined utilizing three parameters in a triangle format (PC, GGBFS and MP)

Table 3. *Ratios of the parameters in the compositions under study*

nº	PC	GGBFS	MP
1	0	0	1
2	0	0.25	0.75
3	0	0.50	0.50
4	0	0.75	0.25
5	0	1	0
6	0.25	0	0.75
7	0.25	0.25	0.50
8	0.25	0.50	0.25
9	0.25	0.75	0
10	0.50	0	0.50
11	0.50	0.25	0.25
12	0.50	0.50	0
13	0.75	0	0.25
14	0.75	0.25	0
15	1	0	0

Fundamental formulation of HPC

In order to ascertain the essential formulation of HPC excluding included air, the Sherbrooke University technique was implemented [1], by following the guidelines provided in the standard [40].The HPC was developed with a target SC of 70 MPa at 28 days. A graph that illustrates the relation among the W/L ratio and the desired SC after 28 days can be used for estimating the W/L ratio. As a result, the ratio is 0.33. In cases where the superplasticizer saturation point is unknown, it is advised to begin with 145 l/m^3 of mixing water. Water is W = 148.5 l/m^3 until an acceptable slump (20 cm) is achieved, which is necessary for the HPC.450 kg/m^3 of cement is the result. In the event that the saturation point is unknown, the superplasticizer dose can always be started at 1% and then increased to 1.5% of binder based on observations made during test batches. The granulometric curves were used in conjunction with the Dreux-Gorisse methodology [41] for enhancing the aggregates granular skeleton. The basic composition of HPC was not altered in the ensuing studies, while the amount of sand and binder changed for every mixture. With fractions of 3/8 mm and 8/12.5 mm, the coarse aggregate ratios (gravels) were 23.08% and 76.92% of the overall volume of the gravels, respectively. To achieve the component total absolute volumes to equal one m^3, the amount of sand in each composition was changed. Table 4 lists the mixtures that have been HPC assessed.

***Table 4**. Examined compositions*

HPC n°	PC (kg/m^3)	GGBFS (kg/m^3)	MP (kg/m^3)	Water (l/m^3)	Sp (kg/m^3)	Sand (kg/m^3)	G (3/8 mm) (kg/m^3)	G (8/12.5 mm) (kg/m^3)
HPC 1	360	0	90			781.90		
HPC 2	360	22.5	67.5			783.92		
HPC 3	360	45	45			785.93		
HPC 4	360	67.5	22.5			787.95		
HPC 5	360	90	0			789.97		
HPC 6	382.5	0	67.5			785.42		
HPC 7	382.5	22.5	45			787.44		
HPC 8	382.5	45	22.5	148.5	6.75	789.45	242.31	807.69
HPC 9	382.5	67.5	0			791.47		
HPC 10	405	0	45			788.94		
HPC 11	405	22.5	22.5			790.96		
HPC 12	405	45	0			792.97		
HPC 13	427.5	0	22.5			792.46		
HPC 14	427.5	22.5	0			794.48		
HPC 15	450	0	0			795.98		

Tests and samples preparation

Approximately fifteen HPC mixes were created and manufactured in the laboratory for this study (Figure 6). After mixing, accurate measurements were obtained using the Abrams cone slump test. The technique outlined in the standard [42] was employed to assess the slump of the various formulations. Once molded into molds, they are covered with plastic sheeting and kept in the laboratory for 24 hours to prevent rapid the evaporation of free water. Following the demolding process, the samples were kept in water saturated with lime at an approximate temperature of 20 ± 2°C until the test day. The second step involves using cubic samples (100 x 100 x 100 mm) in conformity with European standard [43] to conduct compressive strength testing at 7 and 28 days. The measurements average is established following the testing of six samples [44]. Ensuring optimal HPC quality in the cured state requires high compressive strength, which is a crucial measure. The third stage involved using the [45] criteria to determine the water-accessible porosity for the 15 HPCs after 28 days. The process to assess porosity involves drying the samples in an oven at 105°C until they attain a constant weight (M_d). Following that, they are submerged in water during 48 hours, left in a boiling water bath about for 5 hours, and taken out to be weighed in both water and air (M_w and M_{sds}). The porosity accessible to water is provided by Eq. (7):

$$P = 100\left(\frac{Msds - M_d}{Msds - Mw}\right) \tag{7}$$

Where: P (%) is porosity accessible to water; M_{sds} (g): surface-dry saturated sample's mass measured in air; M_d (g): sample dry mass; M_w(g): mass, ascertained by hydrostatic weighing, of the seemingly dry saturated sample weighed in water.

Fig. 6. Photos showing the tests performed

RESULTS

Table 5 presents the findings of the characterization tests performed on the 15 HPCs. With the use of these results, statistical models are created to illustrate the influence of PC, GGBFS, MP, and various possible mixes on every response. The most efficient models should have relatively high coefficients of correlation.

Table 5. *Characterization findings from tests*

HPC nº	Slump (cm)	Strength of compressive SC (MPa)		Weight of sample (kg)	Porosity accessible to water P at 28 days (%)
		SC at 7 days	SC at 28 days		
HPC 1	15	46.10	52.70	2.210	12.80
HPC 2	17	42.15	55.65	2.235	12.20
HPC 3	18	44.30	58.80	2.260	11.80
HPC 4	20	41.80	61.10	2.305	11.00
HPC 5	24	40.40	60.40	2.300	11.10
HPC 6	16	48.20	57.90	2.245	12.00
HPC 7	17	48.70	60.15	2.280	11.40
HPC 8	22	47.45	61.50	2.310	11.00
HPC 9	23.5	44.60	63.35	2.325	10.70
HPC 10	17	49.75	60.00	2.275	11.50
HPC 11	20.5	45.70	63.90	2.320	10.80
HPC 12	22.5	43.75	67.00	2.360	10.10
HPC 13	19	48.00	66.50	2.345	10.30
HPC 14	21.5	45.50	69.25	2.415	09.40
HPC 15	20	48.35	65.10	2.340	10.40

Table 6 displays estimated parameters of the model for the investigated responses. Table 6 indicates that all responses have satisfactory coefficients of correlation ($R^2 \geq 0.76$) and probability values are appropriate for the formed models. A negative value of the parameter suggests a diminished response when it increases. It is essential to remember that a rise in one parameter will result in a decrease in the others as the parameters reflect the ratios of the components that make up the mixture. All coefficients were found utilizing the least-squares process, which involves decreasing the total of residual squares.

Table 6. *Estimates of the assessed responses' model parameters*

Term	Slump		SC_7		SC_{28}		P_{28}	
R^2	0.95		0.76		0.94		0.93	
P	< 0.0001		< 0.0121		< 0.0001		< 0.0001	
Coeff. / P-Value	Coeff.	P-Value	Coeff.	P-Value	Coeff.	P-Value	Coeff.	P-Value
c_1 : (PC)	20.021	<0.0001*	46.982	<0.0001*	66.824	<0.0001*	10.029	<0.0001*
c_2 : (GGBFS)	23.700	<0.0001*	41.032	<0.0001*	60.438	<0.0001*	11.107	<0.0001*
c_3 : (MP)	14.985	<0.0001*	45.304	<0.0001*	52.620	<0.0001*	12.829	<0.0001*
*c_{12} : (PC*GGBFS)*	04.429	0.1509	3.914	0.5525	11.914	0.0464	-2.029	0.0991
*c_{13} : (PC*MP)*	-0.714	0.8058	13.571	0.0611	6.014	0.2740	-0.400	0.7253
*c_{23} : (GGBFS*MP)*	-4.286	0.1630	1.886	0.7730	7.557	0.1773	-1.114	0.3388

Notes: **: significant contribution of parameter in the response variation; R^2: correlation parameter; P: probability; Coeff.: estimated coefficient in the linear model; P-Value: probability that the parameter is negligible (null hypothesis H_0). P-Value < 0.05 indicates that the parameter should be in the prediction model.*

From the plots of observed and predicted values in Figure 7, it appears that the points are distributed within the confines of the confidence curves. This finding indicates a high degree of coherence between the values expected by the model and the experimentally observed findings. To confirm the validity of the models, it is required to analyze the residuals between the observed and predicted responses before employing them.

The residues plots displayed in Figure 8 reveal an arbitrary arrangement of points that correspond to the four different types of responses.

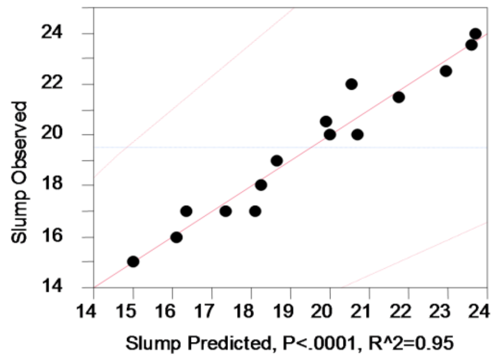

(a) Slump

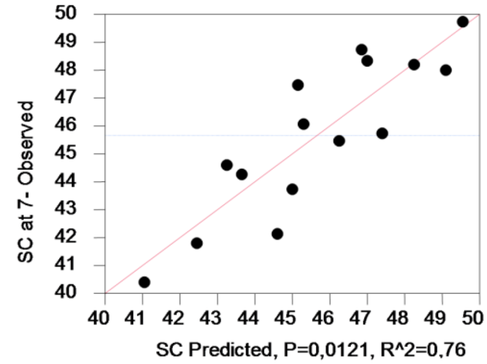

(b) SC at 7-day

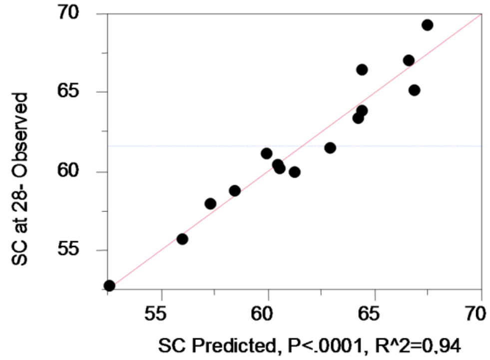

(c) SC at 28-day

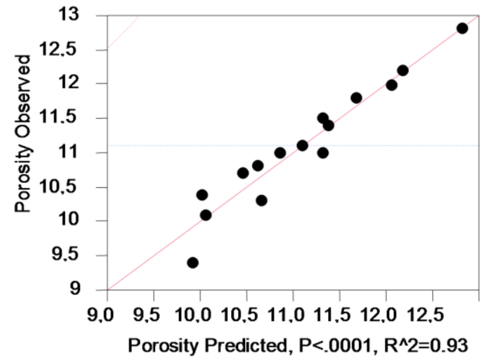

(d) Porosity at 28-day in (%)

Fig. 7. Observed-to-predicted diagrams for: (a) Slump, (b) SC at 7-day, (c) SC at 28-day and (d) P at 28-day

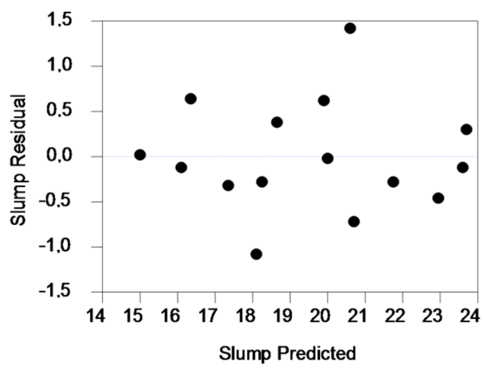

(a) Slump

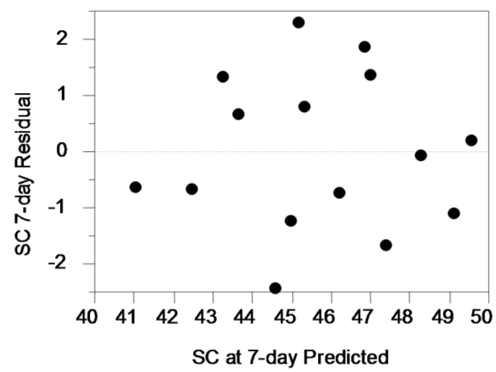

(b) SC at 7-day

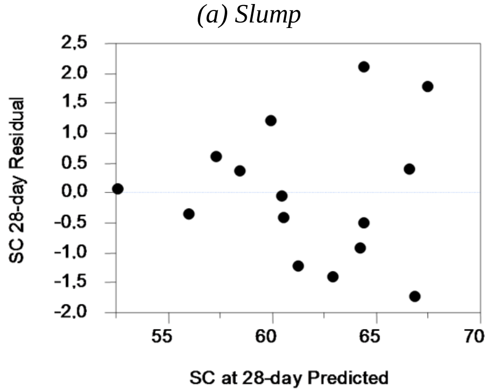

(c) SC at 28-day

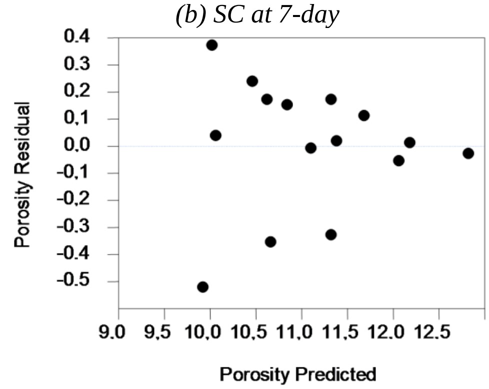

(d) Porosity at 28-day in (%)

Fig. 8. Residues diagrams for: (a) Slump, (b) SC at 7-day, (c) SC at 28-day and (d) P at 28-day

Modeling the slump of HPC

A significant aspect of HPC, which makes it possible to assess how easy it is to implement, is its workability (slump).Predictions for the slump parameter values of the model are displayed in Table 6. The following is a summary of the slump statistical model:

$$Slump\ (cm) = 20.02*PC + 23.70*GGBFS + 14.99*MP + 4.43*PC*GGBFS - 0.71*PC*MP - 4.29*GGBFS*MP \quad (8)$$

The iso-response plots in Figure 9 indicate how the PC, GGBFS and MP ratios influence slump. The findings reveal how the three types and mixtures of factors influence the HPCs workability. Based on the mathematical workability model, the coefficient of each parameter manifestly influences the slump value.

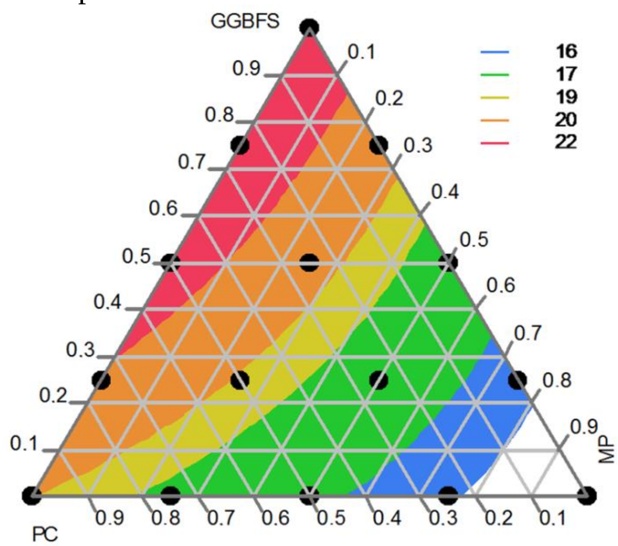

Fig. 9. Slump iso-response curves (cm) as function of PC, GGBFS and MP ratios

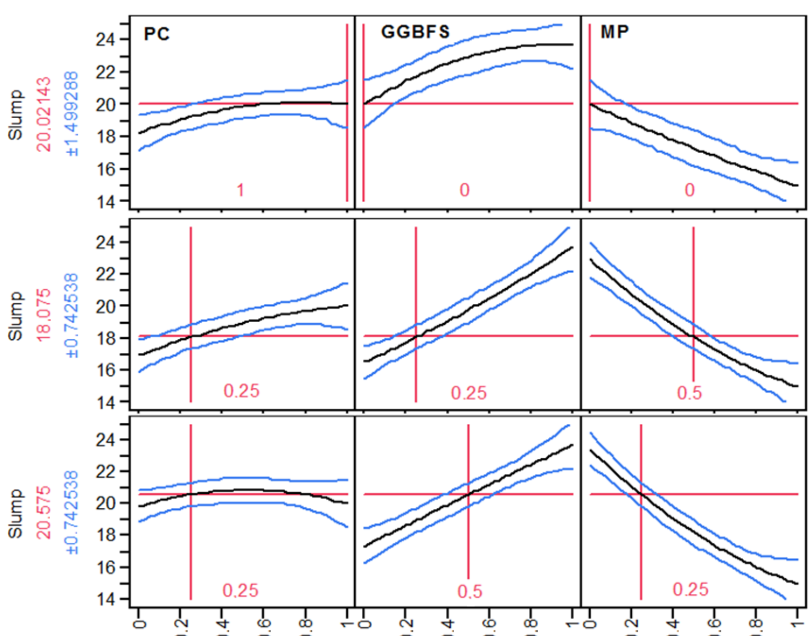

Fig.10. Slump prediction profiler

Additionally, HPCs have acceptable workability values, which vary from 15 to 24 cm. By employing the slump prediction profiler (refer to Figure 10), curves that facilitate comprehension and analysis could be created. Comparing to the reference (HPC 15), it is evident that the presence of GGBFS improves the workability of HPC, especially for the percentage of 100% GGBFS with excellent workability; the addition of PC and GGBFS also enhanced the HPC slump. Researchers can extract as much information as possible from the fewest experiments by employing a prediction profiler. Table 6 and the model indicate that a rise in GGBFS dosage has a major effect on slump, followed by increases in PC and MP dosages and the other accompanying effects. The slump model has a quite high correlation coefficient (R^2 = 0.95).Table 7 displays the LogWorth value which allows us to rank the components according to their order of significance on slump and to comprehend any potential interactions between the effects of the parameters.

Table 7. *Overview of parameters affecting slump*

	LogWorth		P-Value
GGBFS	23.700		<0.0001
PC	20.021		<0.0001
MP	14.986		<0.0001
*PC*GGBFS*	4.429		0.1509
*GGBFS *MP*	-4.286		0.1630
*PC*MP*	-0.714		0.8058

As seen in Figure 9, the rise in the percentage of GGBFS in binary and ternary mixes is responsible for promoting the slump of HPCs. In other words; slump is correlated with the amount of GGBFS present in the mixture. The smooth, glassy texture of the surface and limited water permeability of GGBFS particles make the mix more workable. This finding corresponds to the study [8].On the other hand; the results indicate that the reduction in slump is caused by a rising amount of MP in binary mixes and ternary. Binary mix consisting of 25% PC and 75% GGBFS achieved an acceptable slump value of 23.5 cm. Furthermore, a suitable slump value (22 cm) was reached by a ternary mix HPC 8. The negative values (-4.29) and (-0.71), respectively, indicate that the linked effects (GGBFS*MP) and (PC*MP) have an adverse influence on workability; a decrease in these linked parameters lowers slump. Thus, it is only when the mixture has a small percentage of MP (≤ 25%), the slump can stay decent. Stated otherwise, the effective effect is achieved by adding a modest amount of MP. This is in accordance with the article in the scientific literature [46].

Modeling the compressive strengths of HPC

Since it provides information on the main properties of concrete, compressive strength testing is the most important technique. Additionally, 28-day compressive strength is often the only standard used by the building industry to approve a mixture for use in concrete. The following provides a summary of the 7 and 28-day compressive strength prediction models:

$$SC \text{ at 7-day (MPa)} = 46.98 \cdot PC + 41.03 \cdot GGBFS + 45.30 \cdot MP + 3.91 \cdot PC \cdot GGBFS + 13.57 \cdot PC \cdot MP + 1.89 \cdot GGBFS \cdot MP \quad (9)$$

$$SC \text{ at 28-day (MPa)} = 66.82 \cdot PC + 60.44 \cdot GGBFS + 52.62 \cdot MP + 11.91 \cdot PC \cdot GGBFS + 6.01 \cdot PC \cdot MP + 7.56 \cdot GGBFS \cdot MP \quad (10)$$

Table 6 shows that the prediction models for strengths of compressive provide reasonable correlation values (R^2 = 0.76) at 7 days along with excellent correlation values (R^2 = 0.94) at 28 days. Based on the model and the LogWorth value displayed in Table 8, an increase in PC amount has the greatest impact on SC at 7 days. This is followed by MP and GGBFS doses, the effect of (PC*MP), (PC*GGBFS), and finally the impact of (GGBFS*MP).

Table 8. *Overview of parameters influencing SC at 7-day*

	LogWorth		P-Value
PC	46.982		<0.0001
MP	45.304		<0.0001
GGBFS	41.032		<0.0001
*PC*MP*	13.571		0.0611
*PC*GGBFS*	3.914		0.5525
*GGBFS*MP*	1.886		0.7730

The results of the model and Table 9, which presents the LogWorth value, a rise in PC dose has a major impact on SC at 28 days, followed by GGBFS and MP doses, the effect of (PC*GGBFS), (GGBFS*MP), and finally the impact of (PC*MP).

Table 9. *Overview of parameters influencing SC at 28-day*

	LogWorth		P-Value
PC	66.824		<0.0001
GGBFS	60.438		<0.0001
MP	52.620		<0.0001
*PC*GGBFS*	11.914		0.0464
*GGBFS*MP*	7.557		0.1773
*PC*MP*	6.014		0.2740

Iso-response plots in Figure 11 show the influences of PC, GGBFS, and MP ratios on strengths of compressive at 7 and 28 days. Different forms of the curves have been seen. With respect to the HPC 15 reference, SC was enhanced by the incorporation of PC and MP at 7 days, as demonstrated by the prediction profiler for strength of compressive (Figure 12), which clearly shows that the presence of MP raises the SC of HPC, especially for a ratio of 50% MP with good SC. Figure 11 indicates that the growing amount of MP in binary mixes and ternary contributes for the enhancement of the SC at 7 days. The reason why HPC containing MP has better early-age compressive strength is because MP has the ability to produce carbo-aluminates, which have binding capability. Short-term enhancements in SC may come from MP's filling function as well as its capacity to generate carbo-aluminates. This aligns with the findings published by other investigators [24,25].

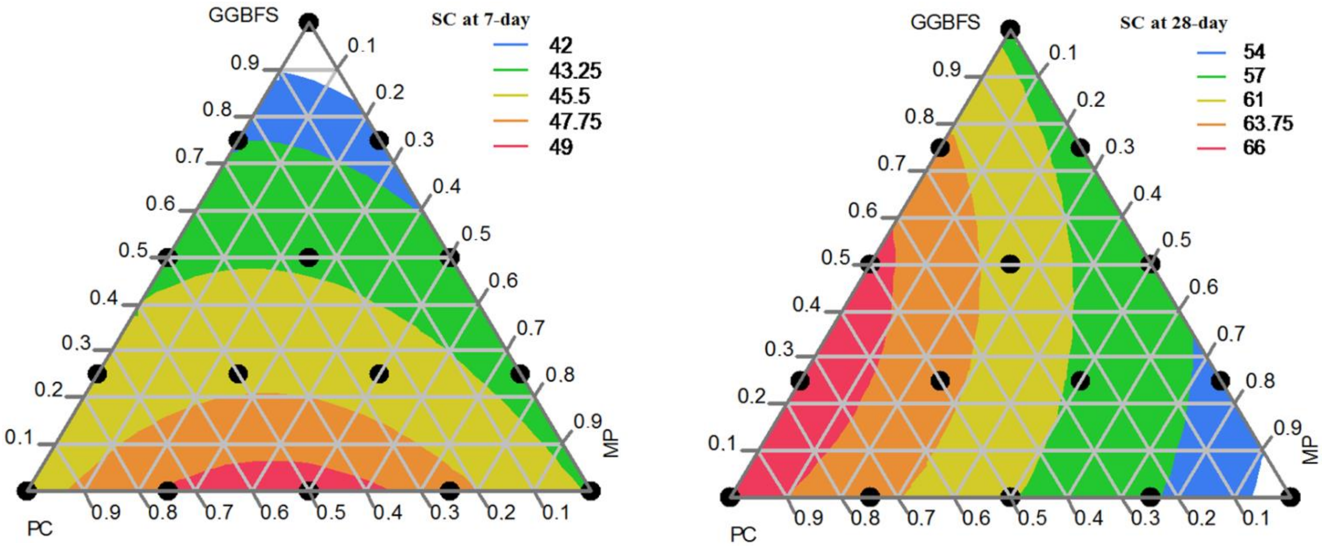

Fig. 11. Compressive strengths (MPa) iso-response curves as function of PC, GGBFS, and MP ratios

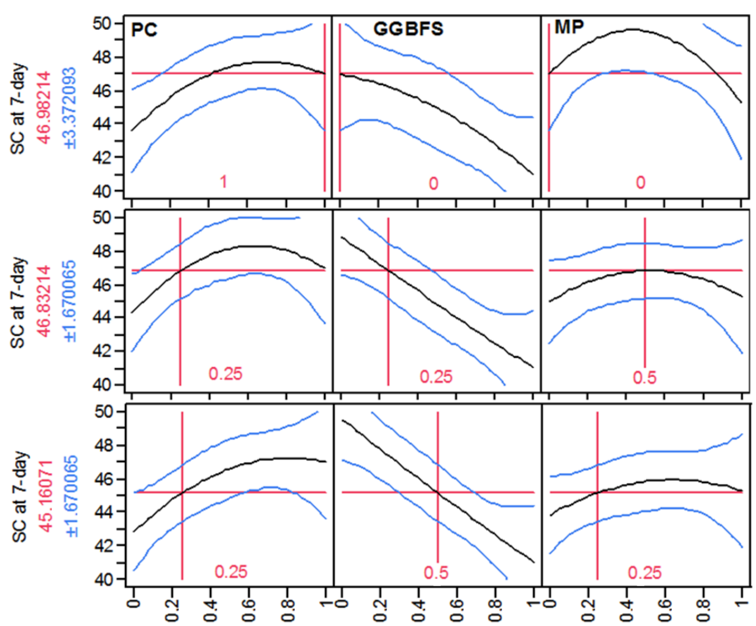

Fig. 12. 7-day SC prediction profiler

A binary mix (50% PC + 50% MP) has been found to have a highest compressive strength of around 49.75 MPa after 7 days; a ternary mix HPC 7 might have a compressive strength of roughly 48.70 MPa. On the other hand, the findings indicate that a little drop in the SC after 7 days is caused by an increasing amount of GGBFS in binary and ternary mixes. This is primarily because GGBFS has a gradual process of hydration and as, due to its pozzolanic reaction, it keeps contributing to hydration beyond 28 days, enhancing a long-term strength [47].Using the compressive strength prediction profiler at 28 days (refer to Figure 13); it is evident that the inclusion of PC increases the SC of HPC.

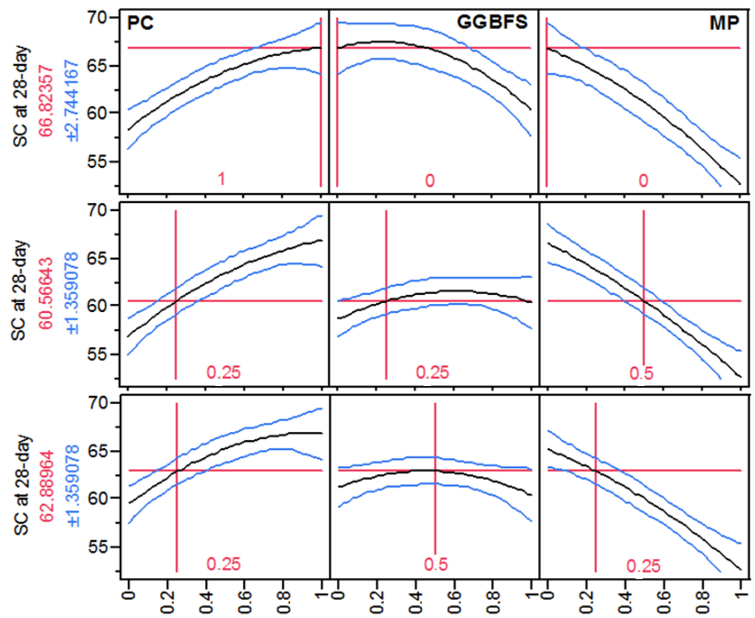

Fig. 13. 28-day SC prediction profiler

This is especially true for the 75% of PC that have an excellent SC, when compared to the reference (HPC 15). The incorporation of PC and GGBFS additionally enhanced the SC. It is clear that using GGBFS by alone led to a minor drop in SC, in comparison with the reference, GGBFS enhanced SC when paired with PC. In this case, the improvement in SC at 28 days is a result of substituting 0.25 of GGBFS for cement. The filler mechanism of GGBFS, the first stage of the GGBFS pozzolanic reaction, and the usage of the proper and suitable mixture of cementitious materials were probably contributing factors to this improvement. These findings are consistent with research [48].Wang et al. [9] state that this decreases porosity and improves the cement paste-aggregate interfacial transition zone. Figure 11 demonstrates that the growing proportion of PC in binary mixes and ternary is responsible for the enhancement in the SC after 28 days. For the binary mix (75% PC + 25% GGBFS), the optimum compressive strength was obtained at 28 days, representing roughly 69.25 MPa; for ternary mix HPC 11, best strength of compressive was approximately 63.90 MPa. On the other hand, the data indicate that a little drop in the SC after 28 days is caused by an increasing quantity of MP in binary mixes and ternary. The phenomenon of pozzolanic reactions dilution provides an explanation for this decrease [46]. As a result, at 28 days, the mixture with a small amount of MP (≤25%) showed higher SC.

Modeling the porosity of HPC

Stronger materials have been known for a long time to have decreasing porosity; cementitious materials in particular exhibit this property. The following describes the porosity prediction model at 28 days:

Porosity at 28-day (%) =
*10.03*PC + 11.11*GGBFS + 12.83*MP- 2.03*PC*GGBFS- 0.40*PC*MP - 1.11*GGBFS*MP* (11)

The model for predicting porosity accessible to water provides a fairly good correlation factor (R^2 = 0.93), as Table 6 shows. Based on the model and Table 10, which indicates the LogWorth importance, an increase in MP dosage has the greatest effect on porosity at 28 days, followed by increases in GGBFS and PC dosage. The porosity has been adversely affected by the linked effects (PC*GGBFS), (GGBFS*MP), and (PC*MP), as indicated by the negative indices (-2.03), (-1.11) and (-0.40), respectively.

Table 10. *Overview of parameters impacting porosity at 28-day*

	LogWorth		P-Value
MP	12.829		<0.0001
GGBFS	11.107		<0.0001
PC	10.029		<0.0001
*PC*GGBFS*	-2.029		0.0991
*GGBFS*MP*	-1.114		0.3388
*PC*MP*	-0.400		0.7253

The porosity at 28 days decreases with a rise in these related factors. The influences of the PC, GGBFS, and MP ratios on the porosity accessible to water at 28 days are shown by the iso-response curves in Figure 14. The findings demonstrate how the three parameters' types and combinations impact the porosity of the HPCs. Utilizing the prediction profiler (refer to Figure 15), it is obvious that the existence of PC decreases the porosity of HPC, this is especially true for the 75% of PC where the porosity is less than that of the reference composition (HPC 15); the combination of PC and GGBFS resulted in this reduction in porosity. Put another way, introducing 25% of GGBFS, instead of cement, helps to reduce porosity after 28 days. This decreased porosity was probably caused by the GGBFS filler mechanism, the hydration of cement, and the first stage of the pozzolanic activity of the GGBFS. Also, as shown by the results of the study [49], the low porosity may also be explained by the products of the GGBFS pozzolanic chemical reaction having a uniform and dense structure. E.g., after 28 days, a low porosity of roughly 10.1% was achieved for a binary mix with ratios of 0.50 PC and 0.50 GGBFS.

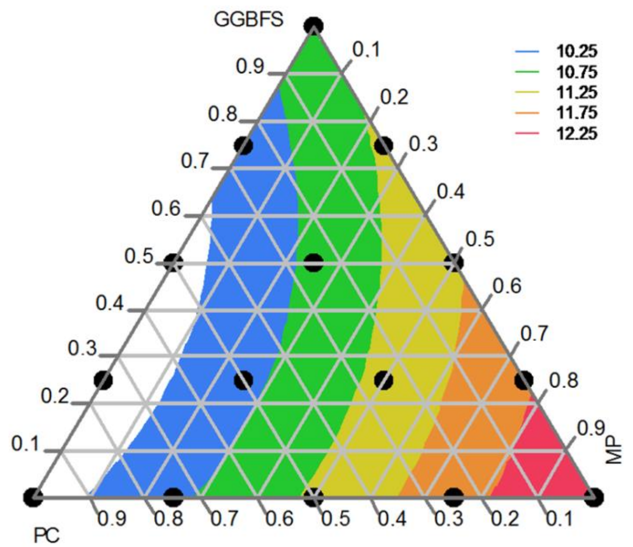

Fig. 14. Porosity at 28-day (%) iso-response curves as function of PC, GGBFS, and MP ratios

Figure 14 illustrates how the growing proportion of PC in binary mixes and ternary can be the cause of the porosity decrease at 28 days. In the binary mix HPC 14, the low porosity was attained at 28 days, representing roughly 9.4%; in the ternary mix HPC 11, it was approximately 10.8%.

Conversely, the findings imply that a modest rise in porosity occurs at 28 days when the MP percentage in binary mixes and ternary increases

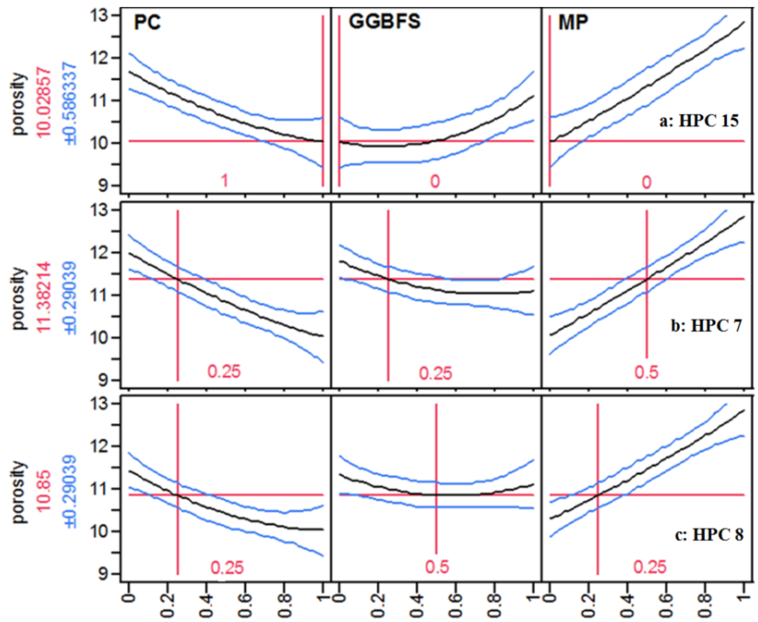

Fig. 15. Porosity prediction profiler at 28-day in (%)

The porosity increased along with the increase in MP substitution percentage. This could occur due to the pore-filling impact caused by MP during optimal substitution [50].Due to this, at 28 days; the porosity is lower in combinations with low MP percentage (≤ 25%). E.g., after 28 days, a binary mix HPC 13 obtained a low porosity of about 10.3%. This drop can be attributed to both MP's filling function and the presence of MP, which promotes the formation of carbo-aluminates. This is in keeping with the results that other researchers have published [24,25].

Finally, Figure 16 illustrates the relationship between porosity accessible to water at 28 days and the compressive strength of HPCs.

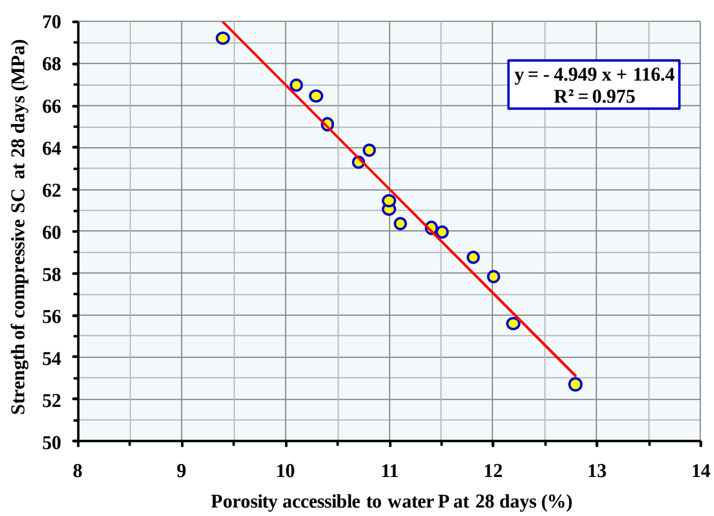

Fig. 16. Relationship between porosity at 28-day and the compressive strength of HPCs

The compressive strength and porosity accessible to water are closely related, displaying an inversely proportional linear relationship and a very strong correlation factor (R^2 = 0.975), indicating that compressive strength improves almost linearly, as porosity decreased. This is consistent with the literature report [11]. The compressive strengths of HPCs at 28 days may be predicted based on the porosity accessible to water, according to this strong relationship.

CONCLUSIONS

The main findings of the scientific paper are listed below:

- Using the statistical analysis, highly accurate models and prediction curves were created for HPC slump, strengths of compressive at 7 and 28 days and porosity accessible to water at 28-day.
- All responses have satisfactory coefficients of correlation ($R^2 \geq 0.76$) for all models.
- Mathematical models developed and the predicted results with the actual data demonstrated an excellent level of agreement, better explaining the experimental findings.
- When GGBFS particles are added to cement, the slump of binary and ternary mixes increases because their surface has a glassy, smooth texture and is less water-permeable. Nevertheless, this only has an impact when mixtures have a small MP percentage (≤ 25%).
- MP's ability to produce carbo-aluminates and filling function may contribute to short-term improvements in SC. On the other hand, data indicate that, in all systems, a minor decrease in SC can be attributed by an increase in the percentage of GGBFS.
- It is clear, after 28 days, that using GGBFS alone caused a little drop in SC; however, when GGBFS and PC were mixed, SC increased in comparison with the composition of reference, and porosity reduced. The cement hydration, the GGBFS pozzolanic reaction's initial stage and the filler role of the material were probably responsible for this enhancement. Conversely, SC is superior with lower porosity, when a small percentage of MP is utilized. This reduction in porosity is due both to the filler role of MP and to the MP presence which promotes the formation of carbo-aluminates. An extremely high correlation factor indicated a strong relationship between porosity and SC.
- The best combination is HPC14, containing 5% GGBFS; this offers an optimal equilibrium among the three qualities. With HPC4's (15%GGBFS + 5%MP) qualities being almost identical to those of the reference HPC15, a lower amount of cement may also be utilized. The study findings justify the possibility of MP and GGBFS as substitutes for cement in the production of reasonably priced and ecologically friendly HPC.

REFERENCES

1. P.C. Aïtcin, J.M. Lessard, The composition and design of high-strength concrete and ultrahigh-strength concrete, Developments in the Formulation and Reinforcement of Concrete, Elsevier, 2019, pp. 171-192. Second Edition), Woodhead Publishing Series in Civil and Structural Engineering.

2. E. Cerro-Prada, R. Pacheco-Torres, F. Varela, Effect of multi-walled carbon nanotubes on strength and electrical properties of cement mortar, Mater. 14 (2021) 79.
3. A. Bahari, A. Sadeghi-Nik, F.U.A. Shaikh, A. Sadeghi-Nik, E. Cerro-Prada, E. Mirshafiei, M. Roodbari, Experimental studies on rheological, mechanical, and microstructure properties of self-compacting concrete containing perovskite nanomaterial, Struct. Concr. 23 (2022) 564-78.
4. ACI 211.4R-08, Guide for selecting proportions for high-strength concrete using Portland cement and other cementitious materials, USA, 2008.
5. A.K. Akhnoukh, Accelerated bridge construction projects using high performance concrete, Case Stud. Constr. Mater. 12 (2020) e00313.
6. Z. Tang, W. Li, V.W.Y. Tam, C. Xue, Advanced progress in recycling municipal and construction solid wastes for manufacturing sustainable construction materials, Resour. Conserv. Recycl.: X. 6 (2020) 100036.
7. B.S. Divsholi, T.Y.D. Lim, S. Teng, Durability properties and microstructure of ground granulated blast furnace slag cement concrete, Int. J. Concr. Struct. Mater. 8 (2014) 157-64.
8. H. Beushausen, M. Alexander, Y. Ballim, Early-age properties, strength development and heat of hydration of concrete containing various South African slags at different replacement ratios, Constr. Build. Mater. 29 (2012) 533-540.
9. J.L. Wang, K.M. Niu, Z.F. Yang, M.K. Zhou, L.Q. Sun, G.J. Ke, Effects of fly ash and ground granulated blast-furnaces slag on properties of high-strength concrete, Key. Eng. Mater. 405-406 (2009) 219-25.
10. S. Liu, Z. Wang, X. Li, Long-term properties of concrete containing ground granulated blast furnace slag and steel slag, Mag. Concr. Res. 66 (2014) 1095-103.
11. H. Trong-Phuoc, S.H. Lanh, V.H. Quan, Experimental investigation on the performance of concrete incorporating fine dune sand and ground granulated blast-furnace slag, Constr. Build. Mater. 347 (2022) 128512.
12. G. Pachideh, M. Gholhaki, Assessment of post-heat behavior of cement mortar incorporating silica fume and granulated blast-furnace slag, J. Struct. Fire Eng. 11 (2020) 221-46.
13. X-Y. Wang and H-S. Lee, Modeling the hydration of concrete incorporating fly ash or slag, Cem. Concr. Res. 40 (2010) 984-96.
14. A.M. Mhaya, G.F. Huseien, A.R. Zainal Abidin, M. Ismail, Long-term mechanical and durable properties of waste tires rubber crumbs replaced GBFS modified concretes, Constr. Build. Mater. 256 (2020) 119505.
15. P. Ganesh and A.R. Murthy, Tensile behaviour and durability aspects of sustainable ultra-high performance concrete incorporated with GGBS as cementitious material, Constr. Build. Mater. 197 (2019) 667-80.
16. J. Ahmad, R. Martínez-García, M. Szelag, J. de-Prado-Gil, R. Marzouki, M. Alqurashi, E.E. Hussein, Effects of steel fibers (SF) and ground granulated blast furnace slag (GGBS) on recycled aggregate concrete, Mater. 14 (2021) 7497.
17. A.A. Ramezanianpour, A. Pilvar, M. Mahdikhani, F. Moodi, Practical evaluation of relationship between concrete resistivity, water penetration, rapid chloride penetration and compressive strength, Constr. Build. Mater. 25 (2011) 2472-9.

18. S. Srikanth, C.B.R. Krishna, T. Srikanth, K.J.N. Sai Nitesh, V. Swamy Nadh, S. Kumar, S. Thanappan, Effect of nano ground granulated blast furnace slag (GGBS) volume % on mechanical behaviour of high-performance sustainable concrete, J. Nanomater. 2022 (2022) 5 pages. https://doi.org/10.1155/2022/3742194.
19. R.B. Oza, M.Z. Kangda, M.R. Agrawal, P.R. Vakharia, D.M. Solanki, Marble dust as a binding material in concrete: A review, Mater. Today Proc. 60 (2022) 421-430.
20. K. Vardhan, R. Siddique, S. Goyal, Strength, permeation and micro-structural characteristics of concrete incorporating waste marble, Constr. Build. Mater. 203 (2019) 45-55.
21. H. Hebhoub, H. Aoun, M. Belachia, H. Houari, E. Ghorbel, Use of waste marble aggregates in concrete, Constr. Build. Mater. 25 (2011) 1167-71.
22. A. Ergün, Effects of the usage of diatomite and waste marble powder as partial replacement of cement on the mechanical properties of concrete, Constr. Build. Mater. 25 (2011) 806-12.
23. O. Boughamsa, H. Hebhoub, L. Kherref, M. Belachia, A. Abdelouahed, R. Chaher, Valorization of marble's waste as a substitute in sand concrete, Adv. Concr. Constr. 9 (2020) 217-25.
24. A. Chawla, K.I. Syed Ahmed Kabeer, A.K. Vyas, Evaluation of strength and durability of lean concrete mixes containing marble waste as fine aggregate, Eur. J. Environ. Civ. Eng. 24 (2020) 1398-413.
25. A.A. Aliabdo, A.M.A. Elmoaty, E.M. Auda, Re-use of waste marble dust in the production of cement and concrete, Constr. Build. Mater. 50 (2014) 28-41.
26. V. Kumar, S. Singla, R. Garg, Strength and microstructure correlation of binary cement blends in presence of waste marble powder. Mater. Today Proc. 43 (2021) 857-62.
27. Y. Wang, J. Xiao, J. Zhang, Z. Duan, Mechanical behavior of concrete prepared with waste marble powder, Sustain. 14 (2022) 4170.
28. H.Y. Aruntaş, M. Gürü, M. Dayı, İ. Tekin, Utilization of waste marble dust as an additive in cement production,Mater. Des.31(2010) 4039-42.
29. V. Corinaldesi, G. Moriconi, T.R. Naik, Characterization of marble powder for its use in mortar and concrete,Constr. Build. Mater. 24(2010) 113-7.
30. C. Karakurt and M. Dumangöz, Rheological and durability properties of self-compacting concrete produced using marble dust and blast furnace slag, Mater. 15 (2022) 1795.
31. A. Yahia, K.H. Khayat, M. Sayed, Statistical modelling of the coupled effect of mix design and rebar spacing on restricted flow characteristics of SCC, Constr. Build. Mater. 37 (2012) 699-706.
32. J. Goupy, L. Creighton, Introduction to design of experiments with JMP examples, 3rd ed., Cary (NC): SAS Institute, 2007, p. 438.
33. J. Goupy, La méthode des plans d'expérience, [The experience plans method], Dunod, Paris, 1988.
34. T. Hadji, S. Guettala, M. Quéneudec, Mix design of high performance concrete with different mineral additions, World J. Eng. 18 (2021) 767-79.
35. H. Ben Salah, B. Dalila, T. Bachir, Using a mixture design method to optimize the behavior of high-performance sand concrete, World J. Eng. 20 (2023) 877-87.
36. R.H. Bogue, in: Chemistry of Portland cement, 2nd ed., Reinhold Publishing Corp, New York (NY), 1955, p. 790.

37. R. Chaid, R. Jauberthie, J. Zeghiche, F. Kherchi, Impact de la poudre de marbre conjuguée au calcaire du CEM II sur la durabilité du béton, Eur. J. Environ. Civ. Eng. 15 (2011) 427-45.

38. K. Arroudj, A. Zenati, M.N. Oudjit, A. Bali, A. Tagnit-Hamou, Reactivity of fine quartz in presence of silica fume and slag, Engineering. 3 (2011) 569-76.

39. J. Goupy, Les plans d'experiences [Design of experiments]. France: Revue MODULAD, Numero 34. 2006.

40. ACI 211.1-91, Standard practice for selecting proportions for normal, heavyweight, and mass concrete. American Concrete Institute, Farmington Hills, Michigan, 1991.

41. G. Dreux, Concretes composition, Techniques de l'Ingenieur 2 (1982) 220.

42. NF P 18-451, Fresh concrete, cone slump tests, French standards, France, 1981.

43. NF EN 12390-3, Essais pour béton durci - Partie 3: résistance à la compression des éprouvettes [Tests for hardened concrete - Part 3: compressive strength of the samples], France, 2012.

44. B. Mezghiche, Laboratory Testing of Construction Materials, Publication Universitaire Biskra, Algerie, 2005, p. 120.

45. NF P 18-459, Concrete - Testing hardened: testing porosity and density, French standards, France, 2010.

46. A. Rana, P. Kalla, L.J. Csetenyi, Sustainable use of marble slurry in concrete, J. Clean. Prod. 94 (2015) 304-11.

47. B. Toufik, B. Bensaid, A. Kheireddine, E. Karim, K. El-Hadj, Prediction of the durability performance of ternary cement containing limestone powder and ground granulated blast furnace slag, Constr. Build. Mater. 209 (2019) 215-21.

48. B. Liu, G. Luo, Y. Xie, Effect of curing conditions on the permeability of concrete with high volume mineral admixtures, Constr. Build. Mater. 167 (2018) 359-71.

49. R.K. Majhi, A.N. Nayak, Production of sustainable concrete utilising high-volume blast furnace slag and recycled aggregate with lime activator, J. Clean. Prod. 255 (2020) 120188.

50. M.A. Rashwan, T.M. Al - Basiony, A.O. Mashaly, M.M. Khalil, Behaviour of fresh and hardened concrete incorporating marble and granite sludge as cement replacement, J. Build. Eng. 32 (2020), 101697.